

# Revisit the isospin violating decays of $X(3872)$

Lu Meng,<sup>1</sup> Guang-Juan Wang,<sup>2</sup> Bo Wang,<sup>3,4,\*</sup> and Shi-Lin Zhu<sup>5,†</sup>

<sup>1</sup>*Ruhr-Universität Bochum, Fakultät für Physik und Astronomie,  
Institut für Theoretische Physik II, D-44780 Bochum, Germany*

<sup>2</sup>*Advanced Science Research Center, Japan Atomic Energy Agency, Tokai, Ibaraki, 319-1195, Japan*

<sup>3</sup>*School of Physical Science and Technology, Hebei University, Baoding 071002, China*

<sup>4</sup>*Key Laboratory of High-precision Computation and Application of Quantum Field Theory of Hebei Province, Baoding 071002, China*

<sup>5</sup>*School of Physics and Center of High Energy Physics, Peking University, Beijing 100871, China*

In this work, we revisit the isospin violating decays of  $X(3872)$  in a coupled-channel effective field theory. In the molecular scheme, the  $X(3872)$  is interpreted as the bound state of  $\bar{D}^{*0}D^0/\bar{D}^0D^{*0}$  and  $D^{*-}D^+/D^-D^{*+}$  channels. In a cutoff-independent formalism, we relate the coupling constants of  $X(3872)$  with the two channels to the molecular wave function. The isospin violating decays of  $X(3872)$  are obtained by two equivalent approaches, which amend some deficiencies about this issue in literature. In the quantum field theory approach, the isospin violating decays arise from the coupling constants of  $X(3872)$  to two di-meson channels. In the quantum mechanics approach, the isospin violating is attributed to wave functions at the origin. We illustrate that how to cure the insufficient results in literature. Within the comprehensive analysis, we bridge the isospin violating decays of  $X(3872)$  to its inner structure. Our results show that the proportion of the neutral channel in  $X(3872)$  is over 80%. As a by-product, we calculate the strong decay width of  $X(3872) \rightarrow \bar{D}^0D^0\pi^0$  and radiative one  $X(3872) \rightarrow \bar{D}^0D^0\gamma$ . The strong decay width and radiative decay width are about 30 keV and 10 keV, respectively, for the binding energy from  $-300$  keV to  $-50$  keV.

## I. INTRODUCTION

In 2003, the observation of  $X(3872)$  [1] launched a new era of hadron spectroscopy. Amounts of candidates of exotic hadrons (beyond the  $q\bar{q}$  mesons and  $qqq$  baryons) were observed in experiments (see Refs. [2–9] for reviews). Among these exotic hadron candidates,  $X(3872)$  is undoubtedly the superstar. One of its most salient features is that the mass coincides exactly with the  $\bar{D}^{*0}D^0/\bar{D}^0D^{*0}$  threshold as  $m_{D^0} + m_{D^{*0}} - m_{X(3872)} = (0.00 \pm 0.18)$  MeV [10], which naturally inspired the molecular interpretations [11–15]. Another important feature of  $X(3872)$  is the large isospin violating decay patterns [16–18],

$$\frac{\mathcal{B}[X \rightarrow J/\psi\pi^+\pi^-\pi^0]}{\mathcal{B}[X \rightarrow J/\psi\pi^+\pi^-]} = 1.0 \pm 0.4 \pm 0.3 \quad \text{Belle,}$$

$$\frac{\mathcal{B}[X \rightarrow J/\psi\omega]}{\mathcal{B}[X \rightarrow J/\psi\pi^+\pi^-]} = \begin{cases} 1.6_{-0.3}^{+0.4} \pm 0.2 & \text{BESIII,} \\ 0.7 \pm 0.3 & \text{B}^+ \text{ events, BABAR,} \\ 1.7 \pm 1.3 & \text{B}^0 \text{ events, BABAR.} \end{cases}$$

The two features can be related to each other. The charged threshold  $D^{*-}D^+/D^-D^{*+}$  is about 8 MeV above the neutral threshold. Since the mass of  $X(3872)$  exactly coincides with the neutral threshold, the mass difference between two thresholds plays a critical role on the different contents of the di-meson components in the molecule which lead to the isospin violating decays.

In the past decades, more and more refined theoretical calculations (e.g. Refs. [19–26]) and experimental analysis (e.g. [27, 28]) were performed to investigate the nature of

$X(3872)$ . Its isospin violating decays which are sensitive to the inner structures are of great interest and have been investigated in different scenarios [13, 29–38]. It is well accepted that the large isospin violation is induced by the mass splitting between charged and neutral channels. However, there are some disagreements on the specific mechanisms even in the same picture. For example, Refs. [32] and [35] provided two different scenarios about the large isospin violating decays of  $X(3872)$  in the molecular model. In Ref. [32], the large isospin violating decays were driven by the mass difference in propagators and amplified by the phase space. The coupling constants of the  $X(3872)$  with the neutral and charged di-meson channels were presumed to satisfy the isospin symmetry. In Ref. [35], the authors stressed that the isospin violating effect arises from the wave function of  $X(3872)$  which is related to the coupling constants [30, 33, 39, 40]. This indicated that the isospin violating decays of  $X(3872)$  were induced by the coupling constants. In this work, we focus on the molecular scheme of  $X(3872)$  and aim to make a comprehensive investigation on the isospin violating decays of  $X(3872)$ . To this end, we will adopt the coupled-channel effective field theory [30, 41] to clarify some conceptional ambiguities about coupling constants, wave function and its value at the origin. In this approach, the cutoff-dependence is eliminated exactly. The same formalism was recently used to exploit the structure of  $T_{cc}^+$  state [42].

The work is organized as follows. In Sec. II, the coupling constants of  $X(3872)$  to two di-meson channels are obtained by solving the Lippmann-Schwinger equations (LSEs). In Sec. III, the Schrödinger equation is adopted to discuss the relation of wave function and coupling constants. In Sec. IV, the isospin violating decays of  $X(3872)$  are analyzed and some disadvantages in literature are clarified. In Sec. V, the decay widths of  $X(3872) \rightarrow \bar{D}^0D^0\pi^0$  and  $X(3872) \rightarrow \bar{D}^0D^0\gamma$  are calculated. In Sec. VI, the main conclusions are summarized briefly. At last, more details about calculating sequential

\* wangbo@hbu.edu.cn, corresponding author

† zhul@pku.edu.cn, corresponding author

decays are presented in Appendix A.

## II. COUPLING CONSTANTS

The dominant decays of the  $X(3872)$  are  $D^0\bar{D}^0\pi^0$  and  $D^{*0}\bar{D}^0$  with the fractions being  $(49^{+18}_{-20})\%$  and  $(37 \pm 9)\%$ , respectively [10]. It couples much stronger with the open-charmed channels (e.g.  $D^{*0}\bar{D}^0$ ) than the hidden-charmed ones (e.g.  $J/\psi\pi^+\pi^-$ ). Therefore, as an approximation, we only consider the interplay of the open-charmed channels to investigate the structure of  $X(3872)$ . The hidden-charmed decays can be driven by the open-charmed components of  $X(3872)$  as illustrated in Fig. 1.

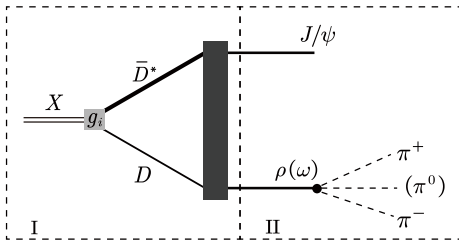


FIG. 1. Isospin violating decays of  $X(3872)$ .

The two closest di-meson thresholds to  $X(3872)$  are the  $\bar{D}^{*0}D^0/\bar{D}^0D^{*0}$  (neutral) and  $D^{*-}D^+/D^-D^{*+}$  (charged) channels with  $m_{D^0} + m_{D^{*0}} - m_{X(3872)} = (0.00 \pm 0.18)$  MeV, while the charged one is located 8 MeV higher. Considering the mass uncertainty, the  $X(3872)$  might be above or below the neutral threshold. In this work, we only focus on the bound state picture as those in Refs. [32, 33, 35]. As a bound state, one can relate the wave function of  $X(3872)$  to its coupling constants with the two di-meson channels. The similar formalism in the work can be extended to resonance states [43, 44].

We use a coupled-channel effective field theory [30, 41] to investigate the  $T$ -matrix of neutral and charged di-meson channels. Similar method has been used to study  $X(3872)$  and  $T_{cc}^+$  states in Refs. [30, 42]. Here, we introduce the formalism briefly. The leading order contact interactions with a hard regulator can be constructed as follows,

$$V(\mathbf{p}, \mathbf{p}') = \begin{bmatrix} v_{11} & v_{12} \\ v_{12} & v_{22} \end{bmatrix} \Theta(\Lambda - p)\Theta(\Lambda - p'), \quad (1)$$

where  $\Theta$  is the step function.  $v_{ij}$  are the energy-independent potentials for the di-meson channels. We use the subscripts 1 and 2 to label the neutral and charged channels, respectively. The coupled-channel LSEs can be reduced to algebraic equations,

$$T(\mathbf{p}, \mathbf{p}') = t\Theta(\Lambda - p)\Theta(\Lambda - p'), \quad t = v + vGt, \quad (2)$$

where  $G = \text{diag}\{G_1, G_2\}$  is the diagonal matrix. The propagator  $G_i$  reads

$$\begin{aligned} G_i(E) &= \int^\Lambda \frac{d^3\mathbf{p}''}{(2\pi)^3} \frac{1}{E - \delta_i - \frac{p''^2}{2\mu} + i\epsilon}, \\ &= \frac{\mu}{\pi^2} \left[ -\Lambda + k_i \arctan \frac{\Lambda}{k_i} \right] \\ &\approx \frac{\mu}{2\pi} \left[ -\frac{2}{\pi} \Lambda + k_i \right], \end{aligned} \quad (3)$$

where  $\delta_1 = 0$  and  $\delta_2 = m_{D^{*+}} + m_{D^-} - m_{D^{*0}} - m_{D^0}$ .  $\mu$  is the reduced mass, for which we neglect the tiny difference between the two di-meson channels.  $k_i \equiv \sqrt{-2\mu(E - \delta_i)}$  is the binding momentum. In Eq. (3), the approximation is a consequence of  $|k_i| \ll \Lambda$ . The  $T$ -matrix corresponding to physical observables are cutoff-independent. The cutoff-dependence in the  $G_i$  is canceled out by the  $v_{ij}$ . To make it clear, we introduce a new set of parameters,

$$\begin{cases} \frac{1}{b_{11}} = \frac{2\pi}{\mu} \left( \frac{v_{22}}{v_{11}v_{22} - v_{12}^2} - G_1 \right) + k_1 \\ \frac{1}{b_{22}} = \frac{2\pi}{\mu} \left( \frac{v_{11}}{v_{11}v_{22} - v_{12}^2} - G_2 \right) + k_2 \\ \frac{1}{b_{12}} = \frac{2\pi}{\mu} \frac{v_{12}}{v_{11}v_{22} - v_{12}^2} \end{cases} \quad (4)$$

Here, the  $b_{ij}$  are the cutoff independent parameters. The solution of LSEs can be expressed as

$$t = \frac{1}{D} \begin{bmatrix} b_{11}b_{12}^2(1 - b_{22}k_2) & b_{11}b_{12}b_{22} \\ b_{11}b_{12}b_{22} & b_{12}^2b_{22}(1 - b_{11}k_1) \end{bmatrix}, \quad (5)$$

with  $D = \frac{\mu}{2\pi} [b_{12}^2(b_{11}k_1 - 1)(b_{22}k_2 - 1) - b_{11}b_{22}]$ .

The bound state corresponds to a pole of the  $T$ -matrix in the real axis. At the pole position, the coupling constants of  $X(3872)$  to two di-meson channels can be approximated by the residues of the  $T$ -matrix,

$$\lim_{E \rightarrow E_0} (E - E_0)t_{ij} = \lim_{E \rightarrow E_0} \left[ \frac{d(t_{ij})^{-1}}{dE} \right]^{-1} = \frac{1}{8M_X^2\mu} g_i g_j, \quad (6)$$

where  $E_0$  and  $M_X$  are the binding energy and mass of  $X(3872)$ , respectively. The coupling constants can be expressed in a very simple form,

$$g_1 = \frac{4M_X\sqrt{\pi\kappa_1}}{\sqrt{\mu}} \cos\theta, \quad g_2 = \frac{4M_X\sqrt{\pi\kappa_2}}{\sqrt{\mu}} \sin\theta, \quad (7)$$

with the following parameters  $\kappa_i$  and  $\theta$

$$\lim_{E \rightarrow E_0} k_i \equiv \kappa_i, \quad \tan^2\theta \equiv \frac{b_{22}\kappa_1(b_{11}\kappa_1 - 1)}{b_{11}\kappa_2(b_{22}\kappa_2 - 1)}. \quad (8)$$

In the calculation, the  $b_{22}$  is eliminated by  $\lim_{E \rightarrow E_0} D = 0$ . The  $\theta$  is actually the mixing angle of two di-meson components in the molecule and will be proved in the latter section.

With a special interaction  $v_{11} = v_{12} = v_{22}$ , our analytical results are in accordance with those in Refs. [32, 33]. What is more important, the cutoff-dependences in the potential  $v_{ij}$  and  $G$  are canceled out in Eq. (4). Our results are

cutoff-independent, which satisfy the renormalization group invariance  $\frac{dT}{d\Lambda} = 0$ . With the extra constraint,  $v_{11} = v_{12} = v_{22}$  [32, 33], the cutoff dependence of  $T$ -matrix can not be eliminated. The assumption  $v_{11} = v_{12} = v_{22}$  is motivated by vanishing interaction in spin triplet channel,  $V_{I=1} = 0$ . However, in the non-perturbative renormalization formalism of LSEs, it is imprudent to introduce the cutoff-independent interaction  $V_{I=1}$ .

### III. WAVE FUNCTIONS

The bound state can be investigated with Schrödinger equation as well. In the coupled-channel effective field theory, the Schrödinger equation reads,

$$(\hat{H}_0 + \hat{V})|\psi\rangle = E_0|\psi\rangle, \quad \hat{V} = \sum_{i,j} \frac{1}{(2\pi)^3} v_{ij} |i\rangle\langle j|, \quad (9)$$

where  $1/(2\pi)^3$  is the normalization factor. In the single-channel framework, the wave function for channel  $|i\rangle$  reads,

$$\phi_i(\mathbf{p}) = \xi_i \frac{\Theta(\Lambda - p)}{E_0 - \frac{p^2}{2\mu} - \delta_i}, \quad \xi_i^2 \approx \frac{\kappa_i}{4\pi^2\mu^2}, \quad (10)$$

where  $\xi_i$  are the normalization constant. The solution of the coupled-channel Schrödinger equation can be introduced as the combination of the single-channel wave functions,

$$\langle \mathbf{p} | \psi \rangle = c_1 \phi_1(\mathbf{p}) |1\rangle + c_2 \phi_2(\mathbf{p}) |2\rangle, \quad (11)$$

where  $c_{1,2}^2$  are the probability of the two components and satisfy  $c_1^2 + c_2^2 = 1$ . The wave function at the origin can be obtained as

$$\begin{aligned} \varphi(0) &= \int \frac{d^3\mathbf{p}}{(2\pi)^{3/2}} \psi(\mathbf{p}) = c_1 \varphi_1(0) |1\rangle + c_2 \varphi_2(0) |2\rangle \\ &= (2\pi)^{3/2} [c_1 \xi_1 G_1 |1\rangle + c_2 \xi_2 G_2 |2\rangle]. \end{aligned} \quad (12)$$

In order to relate the coupling constants with the wave function, we take the approximate  $T$ -matrix near the bound state pole [40]

$$T_{ij}(\mathbf{p}, \mathbf{p}') \approx (2\pi)^3 \frac{\langle \mathbf{p}, i | \hat{V} | \psi \rangle \langle \psi | \hat{V} | \mathbf{p}', j \rangle}{E - E_0}, \quad (13)$$

with  $\langle \mathbf{p}, i | \hat{V} | \psi \rangle$  being calculated by

$$\begin{aligned} \langle \mathbf{p}, i | \hat{V} | \psi \rangle &= \langle \mathbf{p}, i | \hat{H} - \hat{H}_0 | \psi \rangle = \left[ E_0 - \frac{p^2}{2\mu} - \delta_i \right] \langle \mathbf{p}, i | \psi \rangle \\ &= c_i \xi_i \Theta(\Lambda - p). \end{aligned} \quad (14)$$

The  $T$ -matrix reads

$$t_{ij} \approx (2\pi)^3 \frac{c_i c_j \xi_i \xi_j}{E - E_0}. \quad (15)$$

With Eqs. (6) and (7), one can obtain

$$c_1 = \cos \theta, \quad c_2 = \sin \theta. \quad (16)$$

Thus, we can see that the  $\theta$  defined in Eq. (8) is in fact the mixing angle of the charged and neutral channels.

As shown by Eq. (7) and Eq. (12), the coupling constants and wave function at the origin depend on the binding energy (in  $\kappa_i$ ) and mixing angle. The mixing angle reflects the isospin violation effect of  $X(3872)$ .  $\theta = \pi/4$ , and  $-\pi/4$  correspond to the isospin singlet and triplet states, respectively.  $\theta = 0$  stands for  $X(3872)$  as a pure  $\bar{D}^*0 D^0 / \bar{D}^0 D^*0$  bound state.

### IV. MIXING ANGLE AND ISOSPIN VIOLATING DECAYS

The decays  $X \rightarrow J/\psi \pi^+ \pi^- \pi^0$  or  $X \rightarrow J/\psi \pi^+ \pi^-$  can be decomposed into two parts, as shown in Fig. 1. We can define the ratio as,

$$R \equiv \frac{\mathcal{B}^{I=0}(X \rightarrow J/\psi \pi^+ \pi^- \pi^0)}{\mathcal{B}^{I=1}(X \rightarrow J/\psi \pi^+ \pi^-)} = R_1 \times R_2, \quad (17)$$

where  $R_1$  and  $R_2$  represent the ratios for part I and part II as illustrated in Fig. 1, respectively. In part II, the  $J/\psi \rho$  and  $J/\psi \omega$  channels are both located close to the  $X(3872)$ . With the widths of  $\rho$  and  $\omega$  taken into account,  $R_2$  will be suppressed. Based on the formalism of the sequential decays in Appendix A, we can estimate the  $R_2$  as follows [33],

$$\begin{aligned} R_2 &= \frac{\int_{(3m_\pi)^2}^{(m_X - m_{J/\psi})^2} \mathcal{S}(p_V^2, m_\omega, \Gamma_\omega) q(m_X, p_V, m_{J/\psi}) dp_V^2}{\int_{(2m_\pi)^2}^{(m_X - m_{J/\psi})^2} \mathcal{S}(p_V^2, m_\rho, \Gamma_\rho) q(m_X, p_V, m_{J/\psi}) dp_V^2} \\ &\quad \times \frac{\mathcal{B}(\omega \rightarrow \pi^+ \pi^- \pi^0)}{\mathcal{B}(\rho^0 \rightarrow \pi^+ \pi^-)}, \end{aligned} \quad (18)$$

where  $m_i$  and  $\Gamma_i$  are the masses and widths of the  $\rho$  and  $\omega$  mesons.  $p_V$  is the momentum of the  $\rho$  or  $\omega$  in Fig. 1. The  $\mathcal{S}$  and  $q$  are defined as,

$$\mathcal{S}(p_V^2, m_V, \Gamma_V) = \frac{m_V \Gamma_V}{(p_V^2 - m_V^2)^2 + m_V^2 \Gamma_V^2}, \quad (19)$$

$$\begin{aligned} q(M, m_1, m_2) &= \sqrt{[M^2 - (m_1 - m_2)^2][M^2 - (m_1 + m_2)^2]} \\ &= \frac{2M}{2M}. \end{aligned} \quad (20)$$

Eq. (18) is the approximate result which neglects the polarizations of the particles and factors out the  $\omega \rightarrow \pi^+ \pi^- \pi^0$  ( $\rho^0 \rightarrow \pi^+ \pi^-$ ) decay widths (see Appendix A for details). With the experimental results  $\mathcal{B}(\rho^0 \rightarrow \pi^+ \pi^-) \approx 100\%$  and  $\mathcal{B}(\omega \rightarrow \pi^+ \pi^- \pi^0) \approx 89.3\%$  [10], the ratio reads

$$R_2 \approx 0.147. \quad (21)$$

In Ref. [30], the authors did not take approximations mentioned above and obtained  $R_2 = 0.087$  within a refined calculation. We will substitute both the two values of  $R_2$  in the following calculation.

For part I in Fig. 1, there are different scenarios in literature [32, 35]. In our framework, we connect the coupling constants with the wave function. Therefore, we can give a

more comprehensive analysis to clarify the ambiguity in literature. We will interpret the scenarios of Refs. [32, 35] with our notations and then compare them with our approach.

We have two equivalent approaches to investigate the isospin violating decays  $X^{I=a} \rightarrow J/\psi V$  ( $V$  represents the  $\rho$  or  $\omega$  mesons) in part I. The di-meson state  $X^{I=a}$  with isospin  $I = a, I_z = 0$  is composed of the charged and neutral channels as follows,

$$|I = a\rangle = c_{a1}|1\rangle + c_{a2}|2\rangle, \quad (22)$$

where  $c_{ai}$  are the Clebsch-Gordan coefficients. In the quantum field theory, the amplitude can be calculated as

$$\begin{aligned} \mathcal{A}^{I=a}[X \rightarrow J/\psi V] & \\ \sim \int \frac{d^3q}{(2\pi)^3} \frac{\Theta(\Lambda - q)}{E - \frac{q^2}{2\mu}} c_{a1} g_1 + \int \frac{d^3q}{(2\pi)^3} \frac{\Theta(\Lambda - q)}{E - \frac{q^2}{2\mu} - \delta} c_{a2} g_2 & \\ \sim c_{a1} G_1 g_1 + c_{a2} G_2 g_2, & \end{aligned} \quad (23)$$

In the quantum mechanics approach, the transition from  $\bar{D}^*D/\bar{D}D^*$  to  $J/\psi\omega(\rho)$  occurs in very short-range region, because the heavy (anti) quarks have to be reclustered. The transition amplitude is expected to be proportional to the molecular wave function at the origin and reads,

$$\begin{aligned} \mathcal{A}^{I=a}[X \rightarrow J/\psi V] & \sim \sum_{i=1,2} c_{ai} \varphi_i(0) \\ & \sim c_{a1} G_1 g_1 + c_{a2} G_2 g_2, \end{aligned} \quad (24)$$

where  $\varphi_i(0)$  are the wave functions at the origin in Eq. (12). With the above two approaches, we get the same results.

Substituting the specific Clebsch-Gordan coefficients, the ratio  $R_1$  can be calculated as

$$\begin{aligned} R_1 & = \left( \frac{g_1 G_1 - g_2 G_2}{g_1 G_1 + g_2 G_2} \right)^2 \approx \left( \frac{g_1 - g_2}{g_1 + g_2} \right)^2 \\ & = \left( \frac{c_1 \kappa_1^{1/2} - c_2 \kappa_2^{1/2}}{c_1 \kappa_1^{1/2} + c_2 \kappa_2^{1/2}} \right)^2. \end{aligned} \quad (25)$$

Since our framework is independent on the cutoff parameter, one can take the  $\Lambda \gg \kappa_i$  and then can eliminate the  $G_i$  according to Eq. (3).

In Ref. [32], the authors presumed  $g_1 = g_2$ . They had to keep the difference of  $G_1$  and  $G_2$  to make  $R_1$  non-vanishing, which is a cutoff-dependent result. In our approach, with a general interaction (1), the cutoff dependence can be canceled out when  $\Lambda \gg \kappa_i$ . Without constraint of  $v_{11} = v_{22} = v_{12}$  in Ref. [32], the  $g_i$  in Eq. (7) is proportional to the  $c_i$  and  $\kappa_i$ . The coupling constants are determined by the mixing angle of two channels, binding energy and mass differences of two thresholds, which are all physical observables. Therefore, the results in Ref. [32] kept the cutoff-dependent effect from  $G_1$  and  $G_2$  and neglected the more physical effect from  $g_1$  and  $g_2$ . In fact, the coupling constants embed important information about the structure of  $X(3872)$ . In our approach, the drawback of Ref. [32] is cured by introducing more general interaction in Eq. (1) in a framework satisfying the renormalization group invariance.

With the  $R_2$  and  $R_1$  in Eqs. (21) and (25), we can extract the probabilities ( $c_1^2$  and  $c_2^2$ ) of the neutral and the charged channels from the experimental  $R$ . Since the binding energy is unknown, we vary it from 300 keV to 1 keV. In addition to our value of  $R_2 = 0.147$ , we also use the value  $R_2 = 0.087$  in Ref. [30]. By varying the experimental  $R$  from 0.8 to 1.5 [16, 17, 45], we obtain two solutions of  $\tan \theta = c_2/c_1$  for every parameter set. Both solutions are in the range of (0, 1/2). Correspondingly, the mixing angle is in the range of (0,  $\pi/4$ ). The  $c_1^2$  that extracted from the two solutions are presented in Fig. 2. The  $c_1^2$  for the first solution is very close to 1. The second solution of  $c_1^2$  is also larger than 80%, which increases with decreasing the binding energy. Thus,  $X(3872)$  is a bound state dominated by the neutral channel, which has a proportion larger than 80%. In Ref. [38], the calculations in a cutoff-dependent scheme indicated that in the  $X(3872)$ , the weight of the neutral component is (83 – 88)%, which agrees with our results.

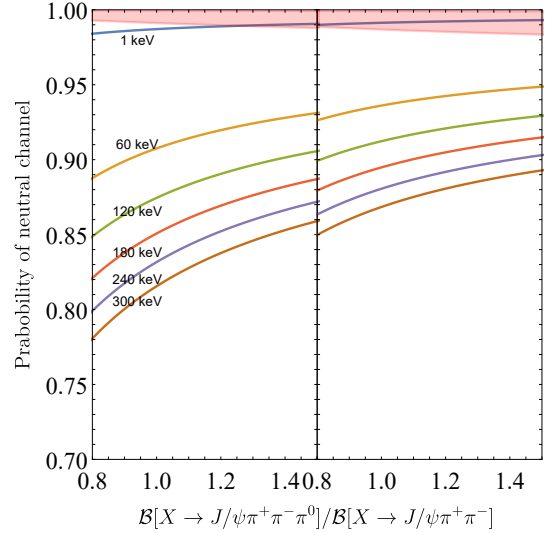


FIG. 2. The probability of the neutral channel in the  $X(3872)$  wave function. In the left and right subfigures, we adopt different  $R_1$  from our calculation and Ref. [30], respectively. We vary the binding energy of  $X(3872)$  from 300 to 1 keV. There are two solutions in each set of input. The first solutions are very close to 1, which are represented by the red shadow. The second solutions are represented by solid lines with the corresponding binding energy near it.

In Ref. [35], the authors obtained a result equivalent to  $R_1 = (c_1 - c_2)^2 / (c_1 + c_2)^2$  in our notation. The amplitude  $X(3872) \rightarrow J/\psi V$  is assumed to be proportional to the coefficients of the related components rather than the wave functions at the origin. The proportions of the neutral channel in Ref. [35] is close to our calculations. However, transition from a  $\bar{D}^*D/\bar{D}D^*$  bound state to the  $J/\psi V$  channel is a short-range process. Taking the ratio of components of wave functions may be still a good approximation for  $R_1$ . But using the wave functions at the origin is more reasonable.

In our previous work [26], we considered the  $D_s \bar{D}_s^* / D_s^* \bar{D}_s$  systems by relating their interaction to the  $DD^* / D^* \bar{D}$  one. But we neglected the coupled-channel effect between them

for the large mass splitting  $\delta_s = D_s^{(*)} - D^{(*)} \approx 100$  MeV.  $X(3872)$  is in the proximity of the  $D\bar{D}^*/D^*\bar{D}$  about several MeVs, which are much smaller than the mass splitting  $\delta_s$ . Thus, it is reasonable to neglect the  $D_s\bar{D}_s^*/D_s^*\bar{D}_s$  channel. In Ref. [32], the authors took the  $D_s\bar{D}_s^*/D_s^*\bar{D}_s$  into consideration in the local hidden gauge approach. The coupling constants were obtained from the residues of the  $T$ -matrix, which implied a sizable fraction of  $D_s\bar{D}_s^*/D_s^*\bar{D}_s$  component. However, one should notice that the conclusion in Ref. [32] is model-dependent. The di-meson interaction derived from the local hidden gauge approach is very strong, which makes the mass splitting  $\delta_s$  play a minor role. Thus, the SU(3) flavor breaking effect is not significant. Meanwhile, the loop diagrams are regularized in dimensional regularization scheme with a varying subtraction coefficient. The solution of  $X(3872)$  can be reproduced by tuning the subtraction coefficient. One can reproduce the pole of  $X(3872)$  without the  $D_s\bar{D}_s^*/D_s^*\bar{D}_s$  channel by choosing a different subtraction coefficient. The coefficient is equivalent to the cutoff parameter in the cut-off regularization scheme. Thus, the conclusion in Ref. [32] is cutoff-dependent.

In Ref. [46], the authors specified processes  $\bar{D}^*D/\bar{D}D^* \rightarrow J/\psi\rho(\omega)$  [“black box” of Fig. 1] by exchanging explicit particles. In principle, the isospin symmetry taken in this work would be a good approximation in the specific mechanism of Ref. [46] as well. One can expect qualitatively consistent conclusions with this work if the similar coupling constants were taken. However, the authors took the the coupling constants in Ref. [32], which included sizable  $D_s\bar{D}_s^*/D_s^*\bar{D}_s$  components. The comparable amplitudes of  $D_s\bar{D}_s^*/D_s^*\bar{D}_s \rightarrow J/\psi\rho$  and  $D_s\bar{D}_s^*/D_s^*\bar{D}_s \rightarrow J/\psi\omega$  will give the considerable isospin violation effect. We should stress that the large proportion of  $D_s\bar{D}_s^*/D_s^*\bar{D}_s$  in  $X(3872)$  is just a model-dependent result.

## V. STRONG AND RADIATIVE DECAYS OF $X(3872)$

With the mixing angle  $\theta$ , we can calculate the strong decay  $X(3872) \rightarrow \bar{D}^0D^0\pi^0$  and radiative decay  $X(3872) \rightarrow \bar{D}^0D^0\gamma$ . In Ref. [47], the authors calculated the two decay widths with the similar interactions in Eq. (1), where the low energy constants are determined by the invariant mass distributions of the  $J/\psi\rho(\omega)$  final states [34] and mass of  $Z_b(10610)$  [48]. In our calculation, we only consider the contribution from the tree diagrams as shown in Fig. 3. The coupling constants between  $X(3872)$  and  $\bar{D}^*D/\bar{D}D^*$  are related to the binding energy and the mixing angle. In this work, we vary the probability of the neutral component of  $X(3872)$  from 80% to 100% and the binding energy from 300 keV to 0 keV, respectively. The vertex  $D^* \rightarrow D\pi$  and  $D^* \rightarrow D\gamma$  are extracted from the experimental widths of  $D^*$ .

The strong decay  $X(3872) \rightarrow \bar{D}^0D^0\pi^0$  is induced by the intermediate neutral  $\bar{D}^{*0}D/D^{*0}\bar{D}$  channel as shown in Fig. 3. The decay vertex  $D^{*0} \rightarrow D^0\pi^0$  is determined by  $D^{*+} \rightarrow D^0\pi^+$  using the isospin symmetry due to the lack of experimental  $D^{*0}$  width. The amplitude of the decay  $D^{*+} \rightarrow D^0\pi^+$  is  $\mathcal{A} = g_\pi q_\pi \cdot \epsilon_{D^*}$ , where  $\epsilon_{D^*}$  and  $q_\pi$  are

the polarization vector of  $D^*$  meson and momentum of pion, respectively. We extract the coupling constant  $g_\pi = 11.25$  as our input.

For the radiative decay, we only list the decay mode  $X(3872) \rightarrow \bar{D}^0D^0\gamma$  in Fig. 3, which is driven by the neutral channel. Another radiative decay mode  $X(3872) \rightarrow D^+D^-\gamma$  should be largely suppressed. On the one hand, it is driven by the charged channel, which only occupies very minor proportion, less than 20%. On the other hand, the leading amplitudes for M1 radiative transitions  $D^{*0,+} \rightarrow D^{0,+}\gamma$  are roughly proportional to the electric charges of the light quarks in the heavy quark limit [49]. The  $D^{*+} \rightarrow D^+\gamma$  is suppressed compared with  $D^{*0} \rightarrow D^0\gamma$ . Thus, the partial decay width of the  $X(3872) \rightarrow D^+D^-\gamma$  is very tiny. The radiative decay vertex of  $D^* \rightarrow D\gamma$  can be parameterized as follows,

$$\mathcal{A}[D^* \rightarrow D\gamma] = g_\gamma \epsilon_{\mu\nu\alpha\beta} \epsilon_\gamma^\mu p_{D^*}^\nu p_\gamma^\alpha \epsilon_{D^*}^\beta, \quad (26)$$

where  $g_\gamma$  denotes the effective coupling constant. Its value is extracted from the partial decay width of  $D^{*0} \rightarrow D^0\gamma$ . For the  $D^{*0}$  meson, we take its total width as 60 keV, which approaches to most of the theoretical results, e.g. [49–52].

In Fig. 4, we present the numerical results of the strong decay  $X(3872) \rightarrow \bar{D}^0D^0\pi^0$  and radiative one  $X(3872) \rightarrow \bar{D}^0D^0\gamma$ . The results show that the strong and radiative decay widths are about 30 keV and 10 keV, respectively, when the binding energy is in the range of (-300, -50) keV. Both decay widths keep increasing with the larger  $X(3872)$  mass (larger phase space) until the binding energy is about -50 keV. When the  $X(3872)$  approaches the neutral threshold, the coupling constant  $g_1$  will decrease significantly since it is proportional to the binding momentum. The strong and radiative decay widths then tend to vanish because of small  $g_1$  even with larger phase space.

## VI. SUMMARY

In this work, we revisit the isospin violating decays of  $X(3872)$  with a coupled-channel effective field theory. In the molecular scheme, the  $X(3872)$  is interpreted as the bound state of  $\bar{D}^{*0}D^0/\bar{D}^0D^{*0}$  and  $D^{*-}D^+/\bar{D}^-D^{*+}$  channels. In a cutoff-independent formalism, we relate the coupling constants of  $X(3872)$  to two channels of its wave function. The isospin violating decays of  $X(3872)$  are obtained by two equivalent approaches, which ameliorate the approaches for this issue in literature. In the quantum field theory approach, the isospin violating decays arise from the coupling constants of  $X(3872)$  to two di-meson channels. We show that the driving source of the isospin violating proposed in Ref. [32] is cutoff-dependent. However, the factors (coupling constants) related to the physical observables were neglected. In the quantum mechanics approach, the isospin violating is attributed to wave functions at the origin, which is also different from that in Ref. [35] focusing on the coefficients of different channels. The transition from a  $\bar{D}^*D/\bar{D}D^*$  bound state to the  $J/\psi V$  is a short-range process. Therefore, using the wave function at the origin is more reasonable.

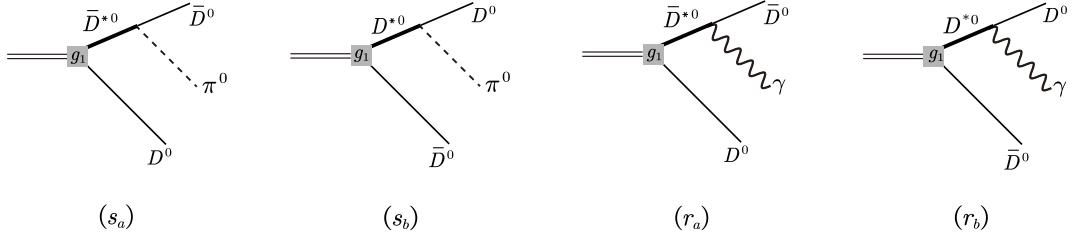


FIG. 3. The Feynman diagrams for strong and radiative decays of the  $X(3872)$  state, where only the neutral channel contributions are illustrated.

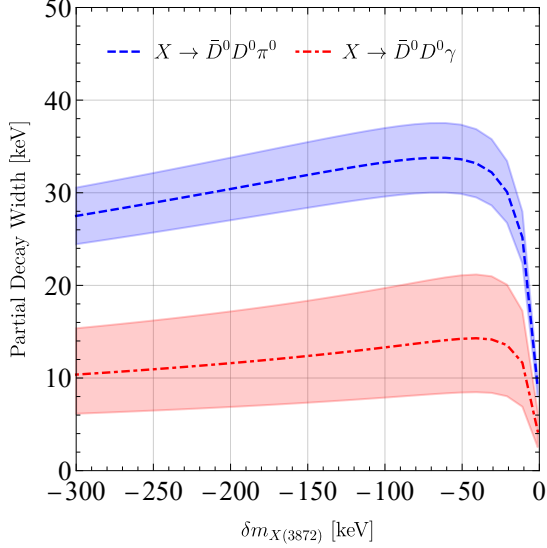


FIG. 4. The partial decay widths of  $X(3872)$  with its binding energy. The shadows represent the probability of the neutral channel in the range (80%, 100%). The central values corresponding to results with 90% neutral component.

Within a comprehensive analysis, we bridge the isospin violating decays of  $X(3872)$  to its structure. Our results show that the proportion of the neutral channel in  $X(3872)$  is over 80%. As a by-product, we calculate the strong decay width of  $X(3872) \rightarrow \bar{D}^0 D^0 \pi^0$  and radiative decay width

$X(3872) \rightarrow \bar{D}^0 D^0 \gamma$ . The strong decay width and radiative decay width are about 30 keV and 10 keV, respectively, for the binding energy from  $-300$  keV to  $-50$  keV.

The isospin violating decays of  $X(3872)$  were investigated in amounts of literature. In this work, we do not aim to provide very refined calculations but try to improve some conceptual understandings.  $X(3872)$  is a benchmark of the exotic hadrons. We hope our work could shed some light on its structure. The approach in Ref. [32] was also adopted to detect the molecular structure of  $P_c(4457)$  [53]. The authors neglected the isospin violating effect in coupling constants but drive the isospin violation by the mass splitting in propagators. The cutoff-dependence in the final results in Ref. [53] can also be improved by the approach in this work.

#### Appendix A: Sequential decay

We use the decay process  $A \rightarrow ab \rightarrow a(123)$  where  $A$  decays into  $a$  and  $b$ , and then  $b$  sequentially decays into three particles to illustrate the calculation of sequential decay. For simplification, we presume  $b$  as a (pseudo)scalar particle and the decay amplitude reads,

$$\mathcal{T} = \mathcal{A}_A[A \rightarrow ab] \frac{i}{p_b^2 - m_b^2 + im_b \Gamma_b} \mathcal{A}_b[b \rightarrow 123], \quad (\text{A1})$$

where  $\mathcal{A}_A$  and  $\mathcal{A}_b$  are the decay amplitudes in sequence. The  $p_b$ ,  $m_b$  and  $\Gamma_b$  are the momentum, mass and width of particle  $b$ , respectively. The differential decay width reads,

$$\begin{aligned} d\Gamma &= \frac{(2\pi)^4}{2M_A} |\mathcal{T}|^2 d\Phi_4 \\ &= \left[ \frac{(2\pi)^4}{2M_A} |\mathcal{A}_A|^2 d\Phi_a \right] \times \left[ \frac{m_b}{(p_b^2 - m_b^2)^2 + m_b^2 \Gamma_b^2} \frac{1}{\pi} dp_b^2 \right] \times \left[ \frac{(2\pi)^4}{2m_b} |\mathcal{A}_b|^2 d\Phi_{123} \right] \\ &\approx \left[ \frac{(2\pi)^4}{2M_A} |\mathcal{A}_A|^2 d\Phi_a \right] \times \left[ \frac{m_b}{(p_b^2 - m_b^2)^2 + m_b^2 \Gamma_b^2} \frac{1}{\pi} dp_b^2 \right] \times \Gamma_{b \rightarrow 123} \\ &= \left[ \frac{(2\pi)^4}{2M_A} |\mathcal{A}_A|^2 d\Phi_a \right] \times \left[ \frac{m_b \Gamma_b}{(p_b^2 - m_b^2)^2 + m_b^2 \Gamma_b^2} \frac{1}{\pi} dp_b^2 \right] \times \mathcal{B}_{b \rightarrow 123}, \end{aligned} \quad (\text{A2})$$

with the general  $n$ -body phase space as

$$d\Phi_n(P; p_1, \dots, p_n) = \delta^4(P - \sum_i p_i) \prod_i \frac{d^3 p_i}{(2\pi)^3 2E_i}. \quad (\text{A3})$$

$P$  and  $p_i$  are the momenta of the initial and final particles, respectively. The 4-body phase space in Eq. (A2) is decomposed

as follows,

$$d\Phi_4 = d\Phi_a(P; p_b, p_a) d\Phi_{123}(p_b; p_1, p_2, p_3) (2\pi)^3 dp_b^2. \quad (\text{A4})$$

In Eq. (A2), the  $\mathcal{A}_b$  and  $\Phi_{123}$  both depend on  $p_b^2$ . However, for the almost on-shell  $b$ , it will be a good approximation to replace the  $p_b^2$  with  $m_b^2$ . Therefore, one can factor out the  $\Gamma_{b \rightarrow 123}$  in Eq. (A2). The above derivation can be easily extended to the sequential decay  $A \rightarrow ab \rightarrow a(12)$  with  $b$  being a vector particle. As shown in Eq. (18), the  $\omega \rightarrow \pi^+\pi^-\pi^0$  ( $\rho^0 \rightarrow \pi^+\pi^-$ ) decay widths are factored out and the polarizations of the particles are neglected.

## ACKNOWLEDGMENTS

We are grateful to the helpful discussions with Prof. Eu-  
logio Oset. L. M. is grateful to the helpful communi-  
cations with Prof. Dian-Yong Chen. This project was sup-  
ported by the National Natural Science Foundation of China  
(11975033 and 12070131001). This project was also funded  
by the Deutsche Forschungsgemeinschaft (DFG, German Re-  
search Foundation, Project ID 196253076-TRR 110). G.J.  
Wang was supported by JSPS KAKENHI (No.20F20026). B.  
Wang is supported by the Youth Funds of Hebei Province (No.  
042000521062) and the Start-up Funds for Young Talents of  
Hebei University (No. 521100221021).

- 
- [1] S. K. Choi *et al.* (Belle), *Phys. Rev. Lett.* **91**, 262001 (2003), [arXiv:hep-ex/0309032](#).
- [2] H.-X. Chen, W. Chen, X. Liu, and S.-L. Zhu, *Phys. Rept.* **639**, 1 (2016), [arXiv:1601.02092 \[hep-ph\]](#).
- [3] A. Esposito, A. Pilloni, and A. D. Polosa, *Phys. Rept.* **668**, 1 (2017), [arXiv:1611.07920 \[hep-ph\]](#).
- [4] R. F. Lebed, R. E. Mitchell, and E. S. Swanson, *Prog. Part. Nucl. Phys.* **93**, 143 (2017), [arXiv:1610.04528 \[hep-ph\]](#).
- [5] A. Hosaka, T. Iijima, K. Miyabayashi, Y. Sakai, and S. Yasui, *PTEP* **2016**, 062C01 (2016), [arXiv:1603.09229 \[hep-ph\]](#).
- [6] F.-K. Guo, C. Hanhart, U.-G. Meißner, Q. Wang, Q. Zhao, and B.-S. Zou, *Rev. Mod. Phys.* **90**, 015004 (2018), [arXiv:1705.00141 \[hep-ph\]](#).
- [7] S. L. Olsen, T. Skwarnicki, and D. Zieminska, *Rev. Mod. Phys.* **90**, 015003 (2018), [arXiv:1708.04012 \[hep-ph\]](#).
- [8] Y.-R. Liu, H.-X. Chen, W. Chen, X. Liu, and S.-L. Zhu, *Prog. Part. Nucl. Phys.* **107**, 237 (2019), [arXiv:1903.11976 \[hep-ph\]](#).
- [9] N. Brambilla, S. Eidelman, C. Hanhart, A. Nefediev, C.-P. Shen, C. E. Thomas, A. Vairo, and C.-Z. Yuan, *Phys. Rept.* **873**, 1 (2020), [arXiv:1907.07583 \[hep-ex\]](#).
- [10] P. A. Zyla *et al.* (Particle Data Group), *PTEP* **2020**, 083C01 (2020).
- [11] M. B. Voloshin, *Phys. Lett. B* **579**, 316 (2004), [arXiv:hep-ph/0309307](#).
- [12] E. S. Swanson, *Phys. Lett. B* **588**, 189 (2004), [arXiv:hep-ph/0311229](#).
- [13] N. A. Tornqvist, *Phys. Lett. B* **590**, 209 (2004), [arXiv:hep-ph/0402237](#).
- [14] S. Fleming, M. Kusunoki, T. Mehen, and U. van Kolck, *Phys. Rev. D* **76**, 034006 (2007), [arXiv:hep-ph/0703168](#).
- [15] Y.-R. Liu, X. Liu, W.-Z. Deng, and S.-L. Zhu, *Eur. Phys. J. C* **56**, 63 (2008), [arXiv:0801.3540 \[hep-ph\]](#).
- [16] K. Abe *et al.* (Belle), in *22nd International Symposium on Lepton-Photon Interactions at High Energy (LP 2005)* (2005) [arXiv:hep-ex/0505037](#).
- [17] P. del Amo Sanchez *et al.* (BaBar), *Phys. Rev. D* **82**, 011101 (2010), [arXiv:1005.5190 \[hep-ex\]](#).
- [18] M. Ablikim *et al.* (BESIII), *Phys. Rev. Lett.* **122**, 232002 (2019), [arXiv:1903.04695 \[hep-ex\]](#).
- [19] V. Baru, A. A. Filin, C. Hanhart, Y. S. Kalashnikova, A. E. Kudryavtsev, and A. V. Nefediev, *Phys. Rev. D* **84**, 074029 (2011), [arXiv:1108.5644 \[hep-ph\]](#).
- [20] V. Baru, E. Epelbaum, A. A. Filin, C. Hanhart, U. G. Meißner, and A. V. Nefediev, *Phys. Lett. B* **726**, 537 (2013), [arXiv:1306.4108 \[hep-ph\]](#).
- [21] L. Zhao, L. Ma, and S.-L. Zhu, *Phys. Rev. D* **89**, 094026 (2014), [arXiv:1403.4043 \[hep-ph\]](#).
- [22] V. Baru, E. Epelbaum, A. A. Filin, J. Gegelia, and A. V. Nefediev, *Phys. Rev. D* **92**, 114016 (2015), [arXiv:1509.01789 \[hep-ph\]](#).
- [23] M. Schmidt, M. Jansen, and H. W. Hammer, *Phys. Rev. D* **98**, 014032 (2018), [arXiv:1804.00375 \[hep-ph\]](#).
- [24] F.-K. Guo, *Phys. Rev. Lett.* **122**, 202002 (2019), [arXiv:1902.11221 \[hep-ph\]](#).
- [25] E. Braaten, L.-P. He, and J. Jiang, *Phys. Rev. D* **103**, 036014 (2021), [arXiv:2010.05801 \[hep-ph\]](#).
- [26] L. Meng, B. Wang, and S.-L. Zhu, *Sci. Bull.* **66**, 1413 (2021), [arXiv:2012.09813 \[hep-ph\]](#).
- [27] R. Aaij *et al.* (LHCb), *Phys. Rev. D* **92**, 011102 (2015), [arXiv:1504.06339 \[hep-ex\]](#).
- [28] R. Aaij *et al.* (LHCb), *Phys. Rev. D* **102**, 092005 (2020), [arXiv:2005.13419 \[hep-ex\]](#).
- [29] M. Suzuki, *Phys. Rev. D* **72**, 114013 (2005), [arXiv:hep-ph/0508258](#).
- [30] E. Braaten and M. Kusunoki, *Phys. Rev. D* **72**, 054022 (2005), [arXiv:hep-ph/0507163](#).
- [31] P. G. Ortega, J. Segovia, D. R. Entem, and F. Fernandez, *Phys. Rev. D* **81**, 054023 (2010), [arXiv:0907.3997 \[hep-ph\]](#).
- [32] D. Gamermann and E. Oset, *Phys. Rev. D* **80**, 014003 (2009), [arXiv:0905.0402 \[hep-ph\]](#).
- [33] D. Gamermann, J. Nieves, E. Oset, and E. Ruiz Arriola, *Phys. Rev. D* **81**, 014029 (2010), [arXiv:0911.4407 \[hep-ph\]](#).
- [34] C. Hanhart, Y. S. Kalashnikova, A. E. Kudryavtsev, and A. V. Nefediev, *Phys. Rev. D* **85**, 011501 (2012), [arXiv:1111.6241 \[hep-ph\]](#).
- [35] N. Li and S.-L. Zhu, *Phys. Rev. D* **86**, 074022 (2012), [arXiv:1207.3954 \[hep-ph\]](#).
- [36] S. Takeuchi, K. Shimizu, and M. Takizawa, *PTEP* **2014**, 123D01 (2014), [Erratum: *PTEP* 2015, 079203 (2015)], [arXiv:1408.0973 \[hep-ph\]](#).
- [37] Z.-Y. Zhou and Z. Xiao, *Phys. Rev. D* **97**, 034011 (2018), [arXiv:1711.01930 \[hep-ph\]](#).
- [38] Q. Wu, D.-Y. Chen, and T. Matsuki, *Eur. Phys. J. C* **81**, 193 (2021), [arXiv:2102.08637 \[hep-ph\]](#).
- [39] F. Aceti and E. Oset, *Phys. Rev. D* **86**, 014012 (2012), [arXiv:1202.4607 \[hep-ph\]](#).
- [40] T. Sekihara, *Phys. Rev. C* **95**, 025206 (2017), [arXiv:1609.09496 \[quant-ph\]](#).
- [41] T. D. Cohen, B. A. Gelman, and U. van Kolck, *Phys. Lett. B* **588**, 57 (2004), [arXiv:nucl-th/0402054](#).

- [42] L. Meng, G.-J. Wang, B. Wang, and S.-L. Zhu, *Phys. Rev. D* **104**, 051502 (2021), arXiv:2107.14784 [hep-ph].
- [43] L. Meng, B. Wang, and S.-L. Zhu, *Phys. Rev. D* **102**, 111502 (2020), arXiv:2011.08656 [hep-ph].
- [44] L. Meng, B. Wang, G.-J. Wang, and S.-L. Zhu, *Sci. Bull.* **66**, 1516 (2021), arXiv:2104.08469 [hep-ph].
- [45] M. Ablikim *et al.* (BESIII), *Phys. Rev. Lett.* **112**, 092001 (2014), arXiv:1310.4101 [hep-ex].
- [46] F. Aceti, R. Molina, and E. Oset, *Phys. Rev. D* **86**, 113007 (2012), arXiv:1207.2832 [hep-ph].
- [47] F. K. Guo, C. Hidalgo-Duque, J. Nieves, A. Ozpineci, and M. P. Valderrama, *Eur. Phys. J. C* **74**, 2885 (2014), arXiv:1404.1776 [hep-ph].
- [48] M. Cleven, F.-K. Guo, C. Hanhart, and U.-G. Meißner, *Eur. Phys. J. A* **47**, 120 (2011), arXiv:1107.0254 [hep-ph].
- [49] B. Wang, B. Yang, L. Meng, and S.-L. Zhu, *Phys. Rev. D* **100**, 016019 (2019), arXiv:1905.07742 [hep-ph].
- [50] D. Ebert, R. N. Faustov, and V. O. Galkin, *Phys. Lett. B* **537**, 241 (2002), arXiv:hep-ph/0204089.
- [51] H.-M. Choi, *Phys. Rev. D* **75**, 073016 (2007), arXiv:hep-ph/0701263.
- [52] D. Becirevic and B. Haas, *Eur. Phys. J. C* **71**, 1734 (2011), arXiv:0903.2407 [hep-lat].
- [53] F.-K. Guo, H.-J. Jing, U.-G. Meißner, and S. Sakai, *Phys. Rev. D* **99**, 091501 (2019), arXiv:1903.11503 [hep-ph].